

Necrotizing Enteritis and Hyperammonemic Encephalopathy Associated With Equine Coronavirus Infection in Equids

Veterinary Pathology
1-10
© The Author(s) 2015
Reprints and permission:
sagepub.com/journalsPermissions.nav
DOI: 10.1177/0300985814568683
vet.sagepub.com



F. Giannitti^{1,2}, S. Diab¹, A. Mete¹, J. B. Stanton³, L. Fielding⁴,
B. Crossley¹, K. Sverlow¹, S. Fish¹, S. Mapes⁵, L. Scott⁶,
and N. Pusterla⁵

Abstract

Equine coronavirus (ECoV) is a *Betacoronavirus* recently associated clinically and epidemiologically with emerging outbreaks of pyrogenic, enteric, and/or neurologic disease in horses in the United States, Japan, and Europe. We describe the pathologic, immunohistochemical, ultrastructural, and molecular findings in 2 horses and 1 donkey that succumbed to natural infection with ECoV. One horse and the donkey (case Nos. 1, 3) had severe diffuse necrotizing enteritis with marked villous attenuation, epithelial cell necrosis at the tips of the villi, neutrophilic and fibrinous extravasation into the small intestinal lumen (pseudomembrane formation), as well as crypt necrosis, microthrombosis, and hemorrhage. The other horse (case No. 2) had hyperammonemic encephalopathy with Alzheimer type II astrocytosis throughout the cerebral cortex. ECoV was detected by quantitative polymerase chain reaction in small intestinal tissue, contents, and/or feces, and coronavirus antigen was detected by immunohistochemistry in the small intestine in all cases. Coronavirus-like particles characterized by spherical, moderately electron lucent, enveloped virions with distinct peplomer-like structures projecting from the surface were detected by negatively stained transmission electron microscopy in small intestine in case No. 1, and transmission electron microscopy of fixed small intestinal tissue from the same case revealed similar 85- to 100-nm intracytoplasmic particles located in vacuoles and free in the cytoplasm of unidentified (presumably epithelial) cells. Sequence comparison showed 97.9% to 99.0% sequence identity with the ECoV-NC99 and Tokachi09 strains. All together, these results indicate that ECoV is associated with necrotizing enteritis and hyperammonemic encephalopathy in equids.

Keywords

betacoronavirus, encephalopathy, enteritis, equine coronavirus, horse, hyperammonemia, immunohistochemistry, infectious disease

The Coronaviridae family includes numerous enveloped positive-stranded RNA viruses responsible for enteric, respiratory, or neurologic disease in a variety of mammalian and avian species.³⁸ The family is divided into 2 subfamilies—Coronavirinae and Torovirinae—and the Coronavirinae subfamily contains 4 genera defined on the basis of serologic cross-reactivity and genetic differences: *Alphacoronavirus*, *Betacoronavirus*, *Deltacoronavirus*, and *Gammacoronavirus*.^{40,41} Equine coronavirus (ECoV) is classified within the *Betacoronavirus* genus, along with bovine coronavirus (BCoV; both within the *Betacoronavirus 1* species), porcine hemagglutinating encephalomyelitis virus, mouse hepatitis virus, rat coronavirus (sialodacryoadenitis virus), certain human coronaviruses (eg, OC43 and HKU1),⁴⁴ severe acute respiratory syndrome coronavirus (SARS-CoV), and Middle East respiratory syndrome coronavirus. SARS-CoV and Middle East respiratory syndrome coronavirus have caused epidemics of respiratory disease in humans in the last

¹California Animal Health and Food Safety Laboratory, School of Veterinary Medicine, University of California, Davis, CA, USA

²Veterinary Diagnostic Laboratory, College of Veterinary Medicine, University of Minnesota, Saint Paul, MN, USA

³Department of Veterinary Microbiology and Pathology and Washington Animal Disease Diagnostic Laboratory, College of Veterinary Medicine, Washington State University, Pullman, WA, USA

⁴Loomis Basin Equine Medical Center, Loomis, CA, USA

⁵Department of Medicine and Epidemiology, School of Veterinary Medicine, University of California, Davis, CA, USA

⁶Idaho Equine Hospital, Nampa, ID, USA

Supplemental material for this article is available on the *Veterinary Pathology* website at <http://vet.sagepub.com/supplemental>

Corresponding Author:

Federico Giannitti, INTA Balcarce, Ruta Nacional 226, Km 73.5, Balcarce 7620, Argentina.

Email: fgiannitti@yahoo.com

decade.^{6,11,43} Three members of the *Coronaviridae* cause life-threatening outbreaks of diarrhea and enteritis in pigs. These include transmissible gastroenteritis virus, porcine epidemic diarrhea virus (PEDV; both within the *Alphacoronavirus* genus), and porcine *Deltacoronavirus*.^{2,18,35,45}

ECoV has been detected in young foals with enteric disease in the United States and France.^{15,22} Recently, ECoV has been associated clinically and epidemiologically with emerging outbreaks of pyrogenic and enteric disease in adult horses in Japan^{23,25,26} and anorexia, lethargy, fever, and, less frequently, diarrhea, colic, and neurologic signs in adult horses in the United States.³¹ Additionally, draft horses experimentally inoculated with ECoV developed clinical signs similar to those observed during natural ECoV outbreaks.²⁴ However, the lesions were not characterized either in natural outbreak or in the experimental cases. To the best of our knowledge, there is only 1 published report in which lesions associated with coronavirus infection are described at a neonatal foal.⁵ Our manuscript describes pathologic, immunohistochemical, ultrastructural, and molecular findings in 2 horses and 1 donkey naturally infected with ECoV.

Materials and Methods

Case Histories

Case Nos. 1 and 2 were American miniature horses from the same premise in California. Case No. 1 was a 6-month-old female that presented with acute lethargy, fever, and tachycardia and died within 6 hours from the onset of disease. Case No. 2 was an 11-year-old mare that presented acutely ill 2 days after case No. 1. The initial clinical signs were fever, acute colic, anorexia, and acute neurologic deficits (head pressing, aimless circling, and depression) with severe hyperammonemia (677 $\mu\text{mol/L}$, normal range $\leq 60 \mu\text{mol/L}$). The mare was euthanized after 12 hours because of a lack of response to treatment and poor prognosis. Case No. 3 was a 7-year-old female miniature donkey from Idaho that developed fever, colic, and severe acute neurologic deficits (head pressing, decreased mentation, recumbency, and seizures) and was euthanized. All 3 cases presented in November 2013, shortly after the animals had returned from a show in Texas. More details on the clinical findings and epidemiologic characteristics of the outbreaks from where these 3 cases originated were published elsewhere.¹²

Pathology and Immunohistochemistry

Carcasses of case Nos. 1 and 2 were submitted to the Davis branch of the California Animal Health and Food Safety (CAHFS) Laboratory System, of the University of California, for full necropsy and diagnostic workup. Samples of brain (including most of the cerebrum, hippocampus, brainstem, medulla oblongata, cerebellum, and pineal gland), trachea, thyroid gland, adrenal gland, spleen, liver, thymus, heart, lungs, kidneys, urinary bladder, pancreas, skeletal muscle, diaphragm, tongue, esophagus, stomach, and small and large intestines

were processed routinely and stained with hematoxylin and eosin. Selected sections of intestine in case No. 1 were also stained with tissue Gram's stain. Formalin-fixed sections of small intestine from case No. 3 were referred by 1 of the authors (J.B.S.) to CAHFS and processed for histopathology as described above.

Selected deparaffinized sections of small intestine from all 3 cases were processed for the detection of coronaviral antigen by immunohistochemistry (IHC) using a mouse monoclonal antibody directed against a nucleocapsid epitope of BCoV (clone BC6-4, Research Technology Innovation, Brookings, SD). Briefly, slides were treated with 3% hydrogen peroxide in methanol, and antigen retrieval was accomplished by heating the slides to 121°C, 18 to 21 psi, for 10 minutes in Antigen Decloaker Solution (CB910 M, Biocare Medical, Concord, CA). After the slides returned to ambient pressure and temperature, the monoclonal antibody (dilution 1:5000) was applied for 30 minutes at room temperature. The slides were rinsed, and an anti-mouse HRP-conjugated polymer (K4001, Dako, Carpinteria, CA) was applied for 30 minutes at room temperature. The slides were rinsed, and AEC substrate chromogen (K3464, Dako) was applied for 10 minutes at room temperature. After rinsing, the slides were counterstained with Mayer's hematoxylin. Formalin-fixed paraffin-embedded small intestine and colon from a horse that tested negative for ECoV, BCoV, and camelid respiratory coronavirus (frozen small intestine and colon tissues) by polymerase chain reaction (PCR) as described below were used as negative controls for the IHC. The positive control consisted of colon of a neonatal calf with colitis caused by BCoV.

Virology

ECoV Quantitative PCR and Sequencing. Feces, fresh and frozen tissue samples, and formalin-fixed paraffin-embedded tissue samples from the 3 cases were processed for nucleic acid purification using an automated nucleic acid extraction system (CAS-1820 X-tractor Gene, Corbett Life Science) according to the manufacturer's recommendations, and total RNA was converted to complementary DNA as previously reported.²⁹ All samples were assayed for the presence of the N gene of ECoV by quantitative PCR (qPCR) as previously reported.³¹

A 435-nucleotide segment of the N gene of ECoV was generated for each outbreak strain (obtained from the donkey from Idaho and 1 of the horses from California) to determine phylogenetic relationship according to Zhang et al.⁴⁴ Sequence of both the 5' and 3' ends of a partial segment of the N gene of ECoV were determined using standard sequencing procedures (BigDye Terminator chemistry, ABI 3730, Applied Biosystems, Foster City, CA, USA).

BCoV and Camelid Respiratory Coronavirus PCR. Samples of jejunum from case No. 1 and small intestinal contents from case No. 2 were minced and homogenized in the presence of 2.5-mm zirconia/silica beads and 1.5 ml of denaturation solution (Ambion 8540G, Life Technologies Corp) using a commercial

bead beater at 6500 rpm for 45 seconds. Homogenized tissue was then subjected to RNA extraction using the Ambion MagMAX-96 Viral RNA isolation kit following the manufacturer's recommendation. Camelid respiratory coronavirus PCR was performed using the AgPath-ID One Step RT PCR kit (Life Technologies Corp) and 4 sets of primers to ensure detection of multiple viral genes and the differentiation of the closely related human coronavirus 229E.⁴ BCoV detection was performed using PCR signatures generously provided by Dr Kathy Kurth (Veterinary Diagnostic Laboratory, Madison, WI) using the AgPath ID multiplex kit (Life Technologies Corp). PCR was performed on an ABI 7500 fast thermocycler platform (Life Technologies Corp). These procedures were performed following CAHFS standard operating procedures.

BCoV Direct Fluorescent Antibody Test. Fresh sections of small intestine from case No. 1 were placed in cryomolds, cryoprotected with Tissue-Tek optimum cutting temperature compound (Sakura Finetek Inc, Torrance, CA), frozen at -80°C for a minimum of 4 hours, cryostat sectioned at 8 μm , and processed for coronavirus antigen detection by direct immunofluorescence using a polyclonal bovine fluorescent antibody conjugate directed against BCoV (American Bioresearch Laboratories, Sevierville, TN).

Other Virology Testing. Lung from case No. 1 and a nasal swab from case No. 2 were tested for equine herpesvirus 1 and mammalian influenza viruses by PCR following procedures previously described.^{33,34} Brain from case No. 2 was processed for West Nile virus (*Flavivirus*) by PCR as previously reported.^{17,32}

Electron Microscopy

Sections of formalin-fixed small intestine from case Nos. 1 and 3 were immersed in modified Karnovsky's fixative (50% strength) and postfixed in 1% osmium tetroxide. The tissue was then rinsed in 0.1M sodium cacodylate, dehydrated through a graded ethanol series, transitioned through propylene oxide, and infiltrated and embedded in Eponate-12 epoxy formulation (Eponate-12 epoxy resin, Ted Pella Inc, Redding, CA). Thick sections were stained with toluidine blue, and selected ultrathin sections were examined using a transmission electron microscope (906E, Carl Zeiss, Peabody, MA), as previously described.³⁹ Small intestinal contents and jejunum (tissue) from case No. 1 and colonic contents from case No. 2 were macerated and suspended in distilled water, then cleared by centrifugation for 20 minutes at 2300 rpm. The supernatant was filtered through syringe filters of a descending pore size and then centrifuged for 45 minutes at 55 000 rpm to obtain a pellet. The pellet was resuspended in distilled water, negatively stained with 2% phosphotungstate, applied to a 300-mesh formvar/carbon-coated grid, and examined with the same electron microscope, as previously described.⁴²

Other Ancillary Diagnostic Tests

Bacteriology and Parasitology. Jejunal tissue from case No. 1 was cultured aerobically (sheep blood agar and MacConkey agar) and anaerobically (prereduced *Brucella* blood agar, prereduced phenylethyl alcohol sheep blood agar, and egg yolk agar; Anaerobic Systems, Morgan Hill, CA) at 37°C for 48 hours and also in selective culture medium (cycloserine-cefoxitin-fructose broth, Veterinary Media Services, University of California, Davis) for isolation of *Clostridium difficile* at 37°C for 48 hours. Lung and liver from case No. 1 and liver and urinary bladder from case No. 2 were also processed for aerobic bacterial culture as described above. Jejunal tissue (case No. 1), colonic contents (case No. 2), and feces (all 3 cases) were processed for the detection of *Salmonella* spp by PCR, as previously described.³ Small intestinal and colonic contents from case Nos. 1 and 2, respectively, were processed for the detection of *Clostridium perfringens* structural antigen and alpha, beta, and epsilon toxins and *C. difficile* A/B toxins by specific commercially available capture enzyme-linked immunosorbent assay (ELISA) kits (BIO-X, Brussels, Belgium; and Techlab, Blacksburg, VA, respectively). Additionally, jejunal tissue from case No. 1 was processed for *Yersinia* spp culture as follows: inoculation of 0.5 to 1 g of sample in 5 ml of sterile phosphate buffered saline, refrigeration at 3°C to 5°C (cold enrichment), subcultured weekly for 3 weeks into *Yersinia*-selective agar (CIN agar) and MacConkey agar, with aerobic incubation at 23°C to 26°C for 42 to 48 hours. Feces or colon contents from case Nos. 1 and 2 were also processed routinely for the detection of nematode eggs/coccidia oocysts by fecal flotation test. All the aforementioned bacteriology and parasitology testing was performed as previously described.^{1,10,30}

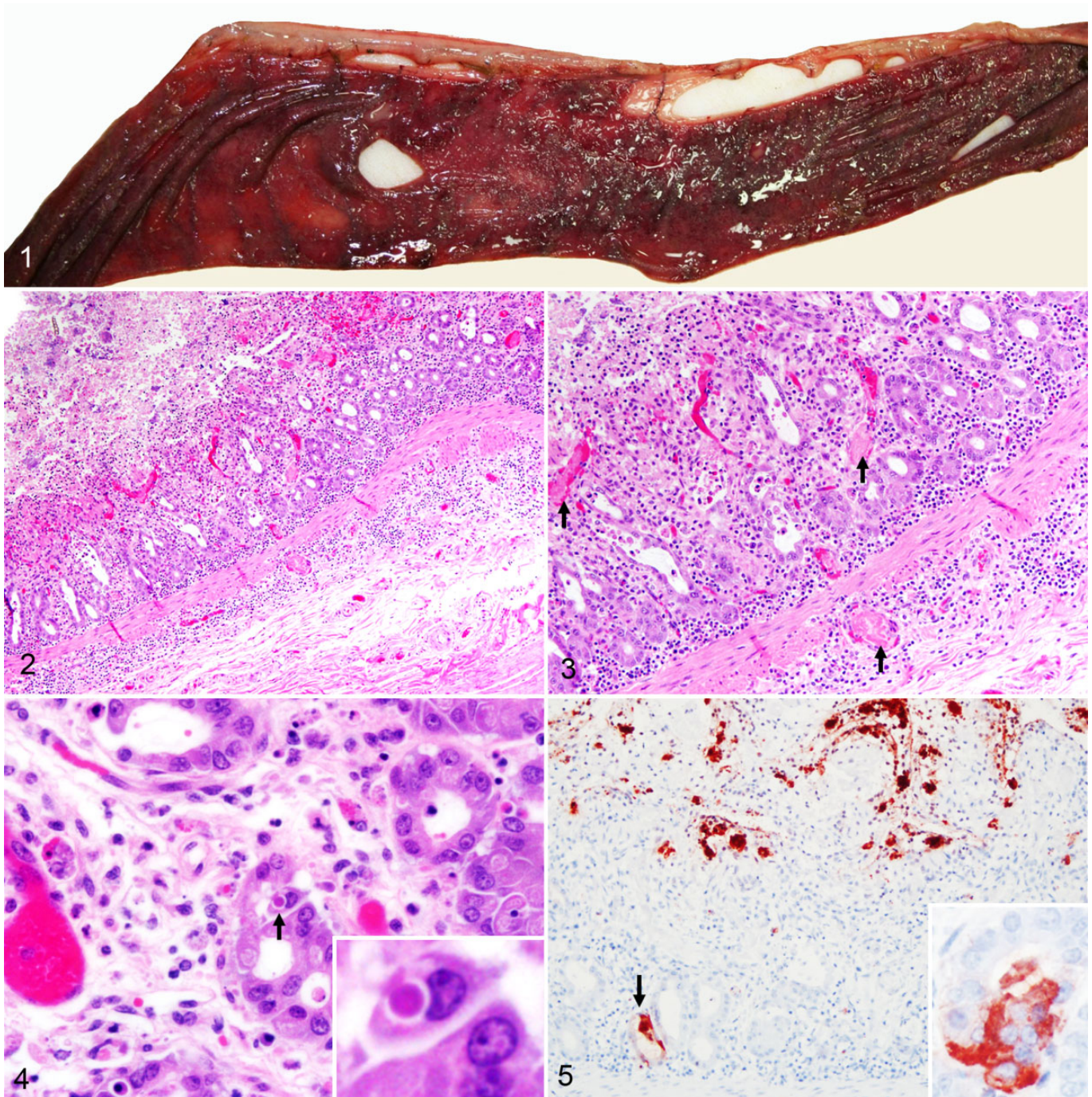
Feces from case Nos. 1, 2, and 3 were also processed for nucleic acid purification as mentioned above (see section on ECoV qPCR) and tested by qPCR for the presence of *Neorickettsia risticii*, *Lawsonia intracellularis*, and *C. difficile* toxin A and B gene as previously described.²⁵

Toxicology. Fresh liver samples from case Nos. 1 and 2 were analyzed for lead, manganese, cadmium, copper, iron, zinc, molybdenum, arsenic, mercury (heavy metal screen), and selenium following procedures previously described.^{20,37} All metal concentrations were estimated on a wet weight basis and compared to reference ranges for horses, following CAHFS standard operating procedures.

Results

Pathology and IHC

Case No. 1 was necropsied shortly after death, and tissues were in a good state of postmortem preservation. The carcass was in good nutritional condition with adequate body fat reserves. Grossly, small intestinal contents were fluid and red tinged. The mucosa of the jejunum and ileum was diffusely reddened and multifocally covered by a thin, friable, finely granular, adherent, brown to gray pseudomembrane (Fig. 1). Microscopically, the



Figures 1–5. Equine coronavirus-associated enteritis, jejunum, horse, case No. 1. **Figure 1.** The mucosa is reddened and covered by a finely granular adherent grayish pseudomembrane (necrotizing enteritis). **Figure 2.** Intestinal villi are shortened, and their tips are necrotic and covered by fibrinous exudate and microhemorrhages. The submucosa is expanded by inflammatory cells and edema. Hematoxylin and eosin (HE). **Figure 3.** Higher magnification of Figure 2. There is loss of crypts, and few remaining crypts are dilated, lined by attenuated epithelium, and contain sloughed necrotic enterocytes. The lamina propria and superficial submucosa are expanded by inflammatory infiltrates. Capillaries and venules in the mucosa and submucosa are occluded by fibrin thrombi (arrows). HE. **Figure 4.** The lamina propria is expanded by edema and inflammatory cells. A crypt enterocyte contains a 3- μ m-diameter round eosinophilic intracytoplasmic inclusion body within a 4- μ m clear vacuole (arrow and inset). HE. **Figure 5.** Diffuse strong granular to globular immunoreactivity associated with necrotic debris at the tip of the necrotic villi (top) and multifocally in the cytoplasm of deep gland enterocytes (arrow and inset). Bovine coronavirus immunohistochemistry.

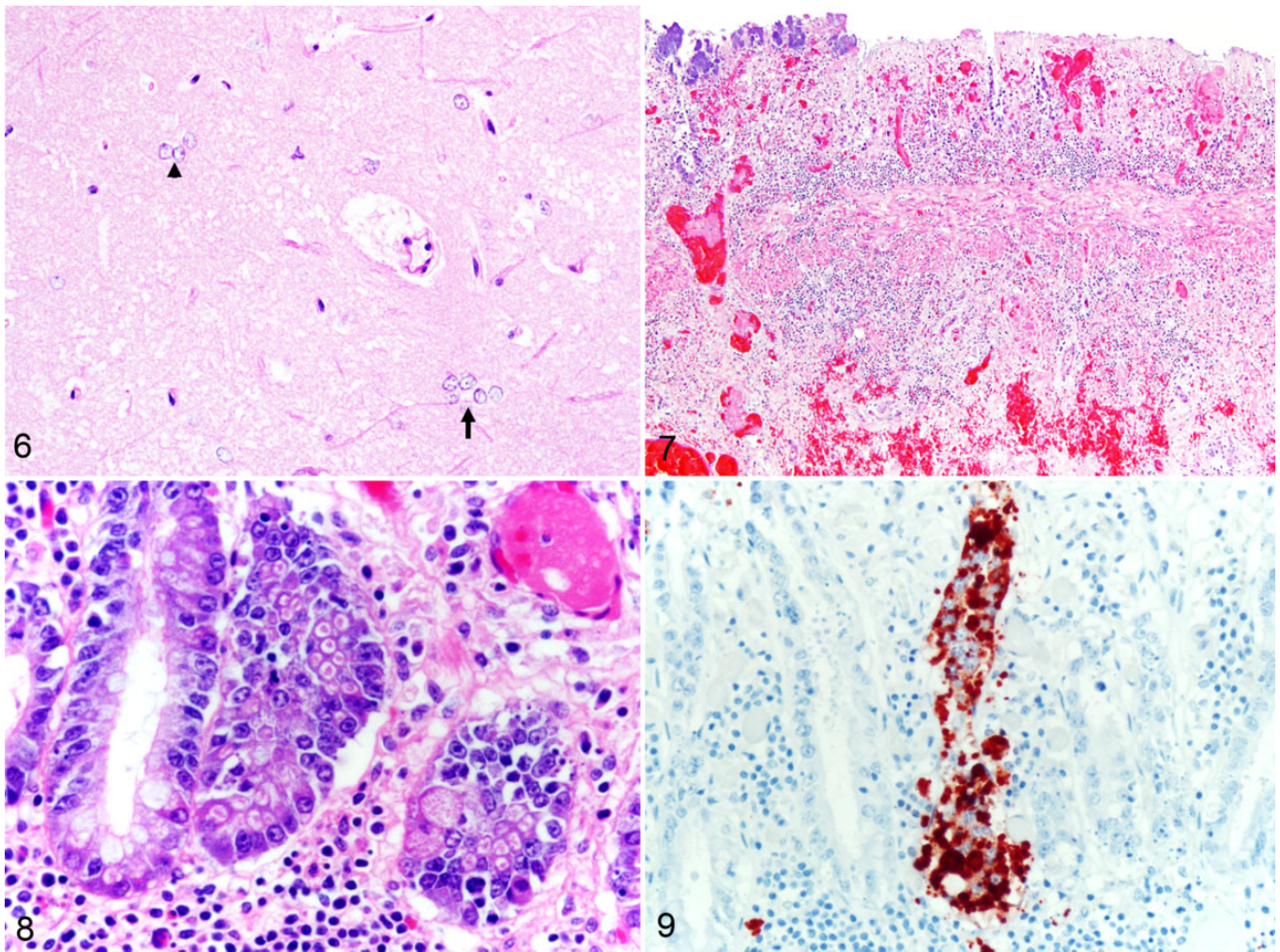
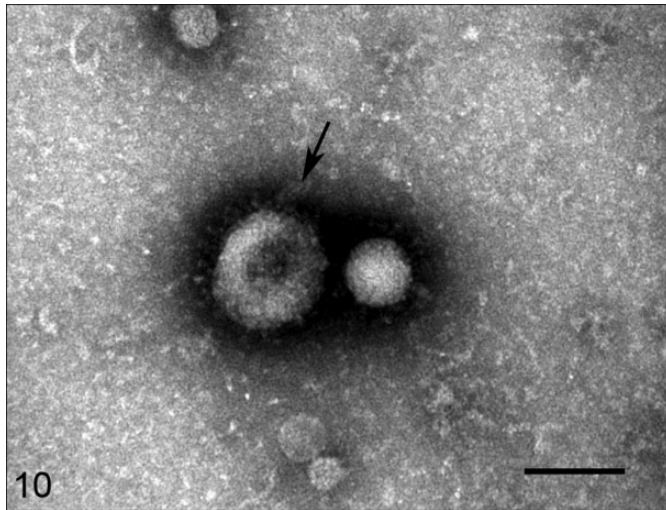


Figure 6. Alzheimer type II astrocyte hypertrophy and hyperplasia (hyperammonemic encephalopathy), cerebral cortex, horse, case No. 2. Cluster of astrocytes with large swollen nucleus and vesicular chromatin are present in the neuropil in groups of 3 (arrowhead) or 5 (arrow) cells. HE. **Figures 7–9.** Equine coronavirus-associated enteritis, jejunum, donkey, case No. 3. **Figure 7.** There is complete loss of glands in the mucosa (ulcerative enteritis) with superficial bacterial colonization and submucosal inflammation, edema, and hemorrhage. Mucosal and submucosal thrombosis is prominent. HE. **Figure 8.** Numerous enterocytes in deep glands contain single irregularly shaped 1.2- to 2- μ m intracytoplasmic eosinophilic inclusion bodies contained in distinct clear vacuoles up to 3.5 μ m. HE. **Figure 9.** Strong granular/globular immunoreactivity in the cytoplasm of deep gland enterocytes. Bovine coronavirus immunohistochemistry.

small intestine, particularly the jejunum and ileum, had severe diffuse necrotizing enteritis characterized by marked villous attenuation; loss of the epithelial lining in the superficial half to two-thirds of the villi; abundant necrotic cellular debris, fibrin, and extravasated erythrocytes (hemorrhage); and few neutrophils overlying the mucosa (pseudomembrane; Fig. 2). There were numerous monomorphic extracellular Gram-negative short bacilli forming colonies and rare individualized Gram-positive bacilli lining the mucosa or within the luminal pseudomembrane. Multifocally, histiocytes, lymphocytes, neutrophils, and eosinophils infiltrated the lamina propria and submucosa. Fibrin thrombi were frequent in the microvasculature (postcapillary venules) of the lamina propria and submucosa. In the deep mucosa, intestinal glands were occasionally destroyed or dilated, filled with necrotic debris and mucus, and lined by flattened or

hypertrophic epithelial cells (“crypt microabscesses”; Fig. 3). Scattered crypt enterocytes contained single 1.5- to 3- μ m-diameter, roughly round intracytoplasmic eosinophilic inclusion bodies contained within clear vacuoles up to 4 μ m in diameter (Fig. 4). In sections of ileum, there was marked lymphocytolysis of the germinal centers of the Peyer’s patches, characterized by pyknotic and karyorrhectic lymphocytes. Coronaviral IHC in the small intestine revealed widespread, multifocal, strong, granular to globular immunoreactivity in the superficial necrotic layer, in the cytoplasm of crypt enterocytes, and in the cytoplasm of unidentified cells within the lamina propria (Fig. 5) and rarely the submucosa.

The large ventral colon had coalescing patches of bright red discoloration of the mucosa that corresponded histologically with acute hemorrhage expanding the lamina propria, but no



Figures 10 and 11. Coronavirus-like particles, jejunum, horse, case No. 1. **Figure 10.** A 112-nm-diameter coronavirus-like particle (arrow), with peplomer-like structures projecting from the surface. Bar = 100 nm. Negatively stained transmission electron microscopy.

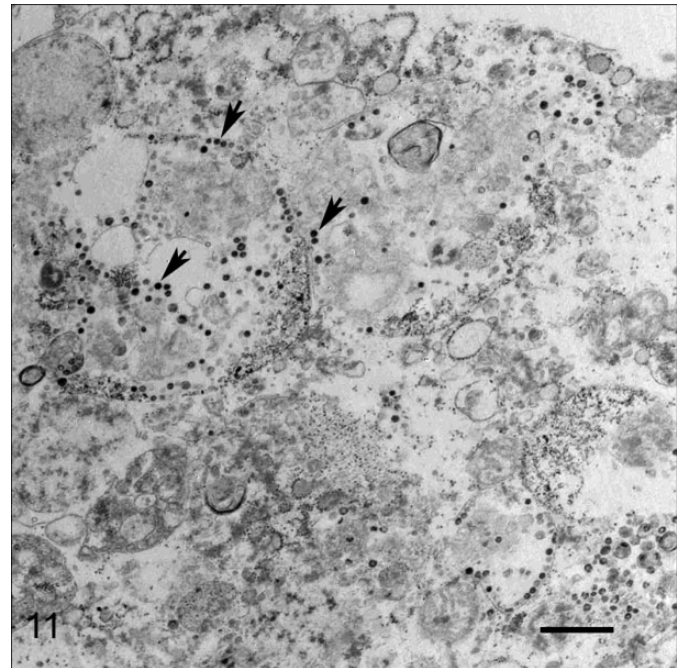


Figure 11. Coronavirus-like particles within the cytoplasm range from 85 to 100 nm in diameter (arrows). Bar = 500 nm. Transmission electron microscopy.

inflammation, necrosis, or other significant lesion was present. Cecal contents were watery, but the mucosa and wall were unremarkable both grossly and microscopically.

Other lesions suggestive of toxemia or sepsis were severe bilateral multifocal hemorrhage of the adrenal glands (the pathologic correlate of the so-called Waterhouse-Friderichsen syndrome), diffuse marked pulmonary congestion and edema, and widespread petechial hemorrhages in the thymus. In the heart, there was focal minimal lymphocytic myocarditis, which was interpreted as an incidental finding. The remainder of the examined organs and tissues was grossly and microscopically unremarkable.

In case No. 2, the carcass was in good nutritional condition. Tissues were in a moderate to advanced state of postmortem decomposition (autolysis), particularly affecting the intestinal tract. This significantly limited the information obtained from the pathologic examination, and it was not possible to reliably assess the presence of microscopic lesions in the intestinal mucosa. However, strong granular to globular coronaviral immunoreactivity was detected infrequently in unidentified cells in the mucosa of the small intestine. Diffusely throughout the cerebral cortex, individual or clusters of 2 to 6 astrocytes in the neuropil were hypertrophied and swollen with prominent nucleus and vesicular chromatin (Alzheimer type II astrocyte hypertrophy and hyperplasia), suggestive of hyperammonemic encephalopathy (Fig. 6).

In case No. 3, the microscopic lesions in the small intestine were similar to those described in the small intestine of case No. 1 but more severe and ulcerative. Multifocal areas in the mucosa had complete loss of enterocytes and glands, and the ulcer bed was lined by necrotic debris and inflammatory cells. The inflammation frequently extended through the submucosa and into the muscularis mucosae and was accompanied by edema and hemorrhage (Fig. 7). Thrombosis and bacterial

colonization of the mucosa and submucosa were frequent. Intracytoplasmic eosinophilic inclusion bodies were frequently observed and often present in many adjacent enterocytes of a same crypt. These inclusions were irregularly shaped, 1.2 to 2 μm , and were contained in clear vacuoles up to 3.5 μm (Fig. 8). The pattern of anti-BCoV immunoreactivity was also similar to that described in case No. 1, with strong granular to globular intracytoplasmic immunoreactivity in gland enterocytes (Fig. 9) and scattered inflammatory cells in the lamina propria. However, no immunoreactivity was found in the submucosa.

In the small intestine of the horse used as a negative control for the anti-BCoV IHC, there was rare multifocal nonspecific granular immunoreactivity aligned along the apical border (brush border) of enterocytes located at the neck of the villi. This pattern was very distinct from the strong globular intracytoplasmic immunoreactivity seen in the positive cases. No immunoreactivity was seen within the cytoplasm of enterocytes, deeper glands, lamina propria, or submucosa in the negative control.

Electron Microscopy

Coronavirus-like particles characterized by spherical, moderately electron-lucent, enveloped virions with distinct peplomer-like structures projecting from the surface were detected by negatively stained electron microscopy of macerated small intestine in case No. 1 (Fig. 10). Electron microscopic examination of small intestinal tissue from case No. 1 revealed many intracytoplasmic particles located in vacuoles and free in the cytoplasm of unidentified (presumably epithelial) cells (Fig.

11). The virions were generally spherical in the range of 85 to 100 nm. No viral particles were detected by electron microscopy from small intestinal or colonic contents in case Nos. 1 and 2, respectively, or from small intestinal tissue in case No. 3.

ECoV qPCR and Sequencing

Results of the ECoV qPCR assay by case and sample type are presented in Supplemental Table 1. Briefly, ECoV nucleic acid was detected in intestinal tissues, contents, and/or feces in all 3 cases and in liver, spleen, and lung in case No. 1. Sequence comparison of a 435-nucleotide segment of the N gene of ECoV showed 100% sequence identity among the virus strains found in 1 of the California mini-horses and the Idaho donkey (case No. 3) and between 97.9% to 99.0% sequence identity with the NC99 and the Tokachi09 strains (GenBank sequence Nos. EF446615, AB555560, AB555559).

Other Diagnostic Tests Results

Results of all the virology, bacteriology, parasitology, and toxicology testing are detailed in Supplemental Table 1. Briefly, coronavirus antigen was detected by fluorescent antibody test using an antibody against BCoV in jejunum of case No. 1, the only case tested by this technique. *Escherichia coli* was isolated in large numbers on aerobic culture from jejunum in case No. 1. *C. perfringens* structural antigen was detected by ELISA in intestinal/colon contents on case Nos. 1 and 2; however, *C. perfringens* toxins alpha, beta, and epsilon were not detected by this method. Small numbers of strongyle eggs were detected in a fecal float in case No. 2. All other diagnostic tests were either negative or unremarkable.

Discussion

ECoV has been associated with emerging outbreaks of fever, anorexia, enteric (diarrhea, colic), and neurologic signs (lethargy) in horses.^{15,23,25,26,31} These reports describe at length the epidemiologic and clinical aspects of ECoV-associated disease in adult horses, which normally presents as a self-limiting problem with high morbidity but low mortality, with most horses recovering in 1 to 4 days with supportive care.³¹ The epidemiologic characteristics, clinical signs, and clinical pathology data of the outbreaks from which the 3 cases presented here originated were recently published elsewhere.¹²

In the absence of Koch's postulates, attributing causality to a potentially new enteropathogen in any animal species is a challenge that requires a multidisciplinary approach. Typically, this begins with elimination of well-known or usual pathogens and is followed by epidemiologic, clinical, pathologic, and microbiological investigations that include a variety of ancillary laboratory tests that altogether support this new association. In case No. 1, tests for most known equine enteropathogens—such as *C. perfringens* type C and *C. difficile* cultures and toxin ELISA; *Salmonella* spp culture and

PCR; *Yersinia* spp culture; *N. risticii*, *Rhodococcus equi*, and *Lawsonia intracellularis* qPCR; and *Streptococcus equi* and *Actinobacillus equuli* cultures were all negative. The epidemiology and clinical investigations were similar to those described in previous outbreaks of ECoV-associated disease, and the pathology was compatible with a viral etiology; thus, ECoV was further investigated.

Multiple testing methods across all 3 cases produced results consistent with ECoV infection. ECoV nucleic acid was detected by qPCR in the small intestine, small intestinal contents, and multiple visceral organs. Electron microscopy identified viral particles compatible with coronavirus in the jejunum. Finally, coronavirus was detected immunologically (direct fluorescent antibody test and IHC) in small intestine using an antibody against BCoV, demonstrating intralesional viral antigen. All together, the results from the 3 cases suggest an association between ECoV infection and the disease process that led to acute onset pyrexia, colic, intestinal, and/or neurologic disease in these equids.

The necrotizing enteritis observed in the foal of case No. 1 and the donkey of case No. 3 was microscopically similar to that reported in syndromes caused by BCoV, including the calf neonatal diarrhea and adult cattle winter dysentery syndromes, but was different from that reported in other well-known enteric diseases induced by coronaviruses, such as the porcine viruses transmissible gastroenteritis virus, PEDV, and porcine *Deltacoronavirus*, all of which are characterized by atrophic (attenuation of superficial enterocytes, villus atrophy, and fusion) rather than necrotizing lesions.^{2,18,45} The intestinal lesions characteristic of BCoV that were observed in case Nos. 1 and 3 include necrosis or sloughing of enterocytes in the apical and lateral portions of the villi with villous attenuation and blunting; dilated crypts that were filled with necrotic and cellular debris and mucus and lined by flattened or hyperplastic epithelium (“crypt microabscesses”); and mucosal inflammation. Additionally, there was pseudomembrane formation, ulceration, submucosal inflammation, mucosal and submucosal hemorrhage, and microthrombosis. These lesions were somewhat similar to the necrotizing lesions described for other common equine enteropathogens, such as *C. perfringens* type C, *C. difficile*, *Salmonella* spp, *N. risticii*, *R. equi*, *Yersinia* spp, *S. equi*, and *A. equuli*.^{2,8–10} However, the presence of crypt necrosis (“crypt microabscesses”) was a distinct feature and should raise suspicion for ECoV.

Case Nos. 1 and 3 showed a few to moderate numbers of roughly round, 1.2- to 3- μ m-diameter eosinophilic intracytoplasmic inclusions surrounded by a clear halo within crypt enterocytes. However, transmission electron microscopy did not show any viral particles within these cytoplasmic inclusions, and further histopathologic and ultrastructural studies are warranted to determine their nature and pathologic significance, if any. Cytoplasmic vacuoles containing eosinophilic proteinic material have been described histologically in the enterocytes of pigs infected with PEDV,³⁵ and coronavirus particles have been demonstrated ultrastructurally within vesicles in the cytoplasm of SARS-CoV-infected human patients.¹⁴

IHC using a mouse monoclonal antibody directed against a nucleocapsid epitope of BCoV was strongly positive in case Nos. 1 and 3 and multifocally, less strongly positive in case No. 2. Given that BCoV was ruled out with a negative BCoV PCR and that ECoV nucleic acid was detected, the immunohistochemical results indicate cross reactivity between BCoV and ECoV, as is predicted based on their sequence similarity and previous results using a pool of monoclonal antibodies against BCoV antigens in a foal with coronavirus-associated enteritis.⁵ A close antigenic relationship between ECoV and BCoV was described upon early characterization of ECoV.¹⁵ The positive IHC in our cases was characterized by strong, granular, intracytoplasmic immunolabeling present on the surface epithelium of the villi and deeper in the crypt epithelium and lamina propria.

Enteric coronavirus infections are generally self-limiting, but viral damage to the intestinal mucosa leading to malabsorption, maldigestion, and loss of the epithelial barrier may lead to secondary complications, such as dehydration, electrolyte alterations, hypoproteinemia, metabolic derangements (hyperammonemia or uremia), septicemia, and toxemia.^{5,25,26,31} In case Nos. 1 and 3, the severe enteric lesions associated with ECoV infection and possible secondary complications likely contributed to the fatal outcome of the disease, as there was no evidence of other disease processes. The identification by qPCR of ECoV in the liver, spleen, and lung of the foal from case No. 1 is suggestive of systemic viral spread. Viremia has been demonstrated for other coronaviruses within the *Betacoronavirus 1* species, such as BCoV.²⁷

Case No. 2 presented with severe hyperammonemia and developed acute neurologic clinical signs compatible with hyperammonemic encephalopathy.¹² The histopathology of the brain was also supportive of hyperammonemic encephalopathy based on the presence of characteristic Alzheimer type II astrocytosis in the cerebral cortex. This lesion is well documented in horses with hepatic or renal encephalopathy.³⁶ Hyperammonemia and encephalopathy in the absence of liver disease have been described in horses with gastrointestinal disease^{7,13,16,28}; thus, the terms “equine enteric hyperammonemia” and “enteric encephalopathy” have been proposed.²¹ Although the exact pathophysiologic mechanisms leading to astrocyte swelling in renal, hepatic, and enteric encephalopathy are not completely understood, the importance of hyperammonemia in the development of this lesion is broadly accepted.^{16,36} Two mechanisms have been suggested to explain the hyperammonemia associated with gastrointestinal disease. One involves the overgrowth of urease-producing bacteria that produce an abundance of ammonia from the degradation of proteins and endogenous urea,¹⁹ while the second involves disruption of the normal intestinal mucosal barrier allowing excessive ammonia absorption from the intestinal lumen into the circulation.⁷ Infectious diseases of the intestinal tract, including *Salmonella* colitis and a case of diarrhea associated with *Clostridium sordellii* infection, have been associated with enteric hyperammonemia,^{7,13} and Alzheimer type II astrocytosis has been described in horses with intestinal disease.¹⁶ In the absence of detectable hepatic and renal disease in case No. 2, we

speculate that hyperammonemia and encephalopathy might have been secondary to intestinal disease. However, as discussed earlier, advanced autolysis in the intestinal tract of this mare hampered the pathologic examination. Case No. 1 did not have neurologic signs or Alzheimer type II astrocytosis suggestive of hyperammonemia, possibly because of the very short clinical course (6 hours), and brain from case No. 3 was not submitted for examination. Ammonia levels in serum were unavailable in case Nos. 1 and 3. ECoV infection should be further investigated as a possible cause of hyperammonemia and enteric encephalopathy in horses, particularly in those without evidence of liver or renal disease and those with idiopathic hyperammonemia.

Previously published epidemiologic data of the outbreaks from which the cases presented in this report originated suggest that the ECoV infection started at the American Miniature Horse Association World Show in Texas in October 2013 and subsequently spread to 2 locations in Idaho and California.¹² Sequence analysis of the ECoV strains obtained from the donkey in Idaho and a horse in California after this show revealed 100% sequence identity, further supporting this hypothesis.

In summary, ECoV infection is associated with naturally occurring necrotizing enteritis in equids, with microscopic lesions somewhat similar to those caused by BCoV in cattle. These lesions need to be distinguished from those described for other common equine enteric pathogens, and ancillary testing is necessary for etiologic confirmation. The causative role and pathogenesis of ECoV in enteric disease and hyperammonemic encephalopathy in equids should be further investigated.

Acknowledgments

The authors thank all the California Animal Health and Food Safety pathology, histology, bacteriology, biotechnology, and toxicology technicians for their assistance.

Declaration of Conflicting Interests

The author(s) declared no potential conflicts of interest with respect to the research, authorship, and/or publication of this article.

Funding

The author(s) received no financial support for the research, authorship, and/or publication of this article.

References

1. Bockemuhl J, Wong JD. Yersinia. In: Murray PR, Baron EJ, Pfaller MA, Jorgensen JH, Tenover FC, Tenover FC, eds. *Manual of Clinical Microbiology*. 8th ed. Washington, DC: American Society of Microbiology Press; 2003:672–683.
2. Brown CC, Baker DC, Barker IK. Alimentary system. In: Maxie MG, ed. *Jubb, Kennedy and Palmer's Pathology of Domestic Animals*. 5th ed. Edinburgh, Scotland: Saunders Elsevier; 2007: 218–220.
3. Cheng CM, Lin W, Van Khahn T, et al. Rapid detection of *Salmonella* in foods using real-time PCR. *J Food Prot*. 2008; **71**:2436–2441.

4. Crossley BM, Mock RE, Callison SA, et al. Identification and characterization of a novel alpaca respiratory coronavirus most closely related to the human coronavirus 229E. *Viruses*. 2012;**4**:3689–3700.
5. Davis E, Rush BR, Cox J, et al. Neonatal enterocolitis associated with coronavirus infection in a foal: a case report. *J Vet Diagnost Invest*. 2000;**12**:153–156.
6. De Groot RJ, Baker SC, Baric RS, et al. Middle East respiratory syndrome coronavirus (MERS-CoV): announcement of the Coronavirus Study Group. *J Virol*. 2013;**87**:7790–7792.
7. Desrochers AM, Dallap BL, Wilkins PA. *Clostridium sordellii* infection as a suspected cause of transient hyperammonemia in an adult horse. *J Vet Intern Med*. 2003;**17**:238–241.
8. Diab SS, Giannitti F, Mete A, et al. Ulcerative enterocolitis and typhlocolitis associated with *Actinobacillus equuli* and *Streptococcus equi* in horses. Paper presented at: American Association of the Veterinary Laboratory Diagnosticians Annual Conference; October 2013; San Diego, CA.
9. Diab SS, Kinde H, Moore J, et al. Pathology of *Clostridium perfringens* type C enterotoxemia in horses. *Vet Pathol*. 2012;**49**:255–263.
10. Diab SS, Rodriguez-Bertos A, Uzal FA. Pathology and diagnostic criteria of *Clostridium difficile* enteric infection in horses. *Vet Pathol*. 2013;**50**:1028–1036.
11. Drosten C, Günther S, Preiser W, et al. Identification of a novel coronavirus in patients with severe acute respiratory syndrome. *N Engl J Med*. 2003;**348**:1967–1976.
12. Fielding CL, Higgins JK, Higgins JC, et al. Disease associated with equine coronavirus infection and high case fatality rate [published online October 15, 2014]. *J Vet Int Med*.
13. Gilliam LL, Holbrook TC, Dechant JE, et al. Postmortem diagnosis of hyperammonemia in a horse. *Vet Clin Pathol*. 2007;**36**:196–199.
14. Goldsmith CS, Tatti KM, Ksiazek TG, et al. Ultrastructural characterization of SARS coronavirus. *Emerg Infect Dis*. 2004;**10**:320–326.
15. Guy JS, Breslin JJ, Breuhaus B, et al. Characterization of a coronavirus isolated from a diarrheic foal. *J Clin Microbiol*. 2000;**38**:4523–4526.
16. Hasel KM, Summers BA, de Lahunta A. Encephalopathy with idiopathic hyperammonemia and Alzheimer type II astrocytes in *Equidae*. *Eq Vet J*. 1999;**31**:478–482.
17. Kleiboeker S, Loiacono C, Rottinghaus A, et al. Diagnosis of West Nile virus infections in horses. *J Vet Diagn Invest*. 2004;**16**:2–10.
18. Madson DM, Magstadt DR, Arruda PH, et al. Pathogenesis of porcine epidemic diarrhea virus isolate (US/Iowa/18984/2013) in 3-week-old weaned pigs. *Vet Microbiol*. 2014;**174**:60–68.
19. Mair TS, Jones RD. Acute encephalopathy and hyperammonemia in a horse without evidence of liver disease. *Vet Rec*. 1995;**137**:642–643.
20. Martin TD, Martin ER, McKee GD, et al. *Method 200.11: Determination of Metals in Fish by Inductively Coupled Plasma-Atomic Emission Spectrometry*. Rev 1.3. Cincinnati, OH: Environmental Monitoring and Support Laboratory; 1987.
21. Milne EM. Equine enteric hyperammonemia: time for a multicenter study? *Vet Clin Pathol*. 2006;**35**:142–143.
22. Miszczak F, Tesson V, Kin N, et al. First detection of equine coronavirus (ECoV) in Europe. *Vet Microbiol*. 2014;**171**:206–209.
23. Narita M, Nobumoto K, Takeda H, et al. Prevalence of disease with inference of equine coronavirus infection among horses stabled in a draft-horse racecourse. *J Jpn Vet Med Assoc*. 2011;**64**:535–539. In Japanese.
24. Nemoto M, Oue Y, Morita Y, et al. Experimental inoculation of equine coronavirus into Japanese draft horses [published online August 20, 2014]. *Arch Virol*.
25. Oue Y, Ishihara R, Edamatsu H, et al. Isolation of an equine coronavirus from adult horses with pyrogenic and enteric disease and its antigenic and genomic characterization in comparison with the NC99 strain. *Vet Microbiol*. 2011;**150**:41–48.
26. Oue Y, Morita Y, Kondo T, et al. Epidemic of equine coronavirus at Obihiro Racecourse, Hokkaido, Japan in 2012. *J Vet Med Sci*. 2013;**75**:1261–1265.
27. Park SJ, Kim GY, Choy HE, et al. Dual enteric and respiratory tropism of winter dysentery bovine coronavirus in calves. *Arch Virol*. 2007;**152**:1885–1900.
28. Peek SF, Divers TJ, Jackson CJ. Hyperammonemia associated with encephalopathy and abdominal pain without evidence of liver disease in four mature horses. *Eq Vet J*. 1997;**29**:70–74.
29. Pusterla N, Kass PH, Mapes S, et al. Surveillance programme for important equine infectious respiratory pathogens in the USA. *Vet Rec*. 2011;**169**:12.
30. Pusterla N, Madigan JE, Leutenegger CM. Real-time polymerase chain reaction: a novel molecular diagnostic tool for equine infectious diseases. *J Vet Intern Med*. 2006;**20**:3–12.
31. Pusterla N, Mapes S, Wademan C, et al. Emerging outbreaks associated with equine coronavirus in adult horses. *Vet Microbiol*. 2013;**162**:228–231.
32. Sandu T, Sidhu D, Dhillon M, et al. Comparison of immunohistochemistry and polymerase chain reaction for detection of West Nile virus in naturally infected dead birds. *J Infect Dev Ctries*. 2010;**4**:587–589.
33. Smith KL, Li Y, Breheny P, et al. Development and validation of a new allelic discrimination real-time PCR assay for the detection of Equine Herpesvirus-1 (EHV-1) and differentiation of A2254 from G2254 strains in clinical specimens. *J Clin Microbiol*. 2012;**50**:1981–1988.
34. Spackman E, Senne DA, Myers TJ, et al. Development of a real-time reverse transcriptase PCR assay for type A influenza virus and the avian H5 and H7 hemagglutinin subtypes. *J Clin Microbiol*. 2002;**40**:3256–3260.
35. Stevenson GW, Hoang H, Schwartz KJ, et al. Emergence of Porcine epidemic diarrhea virus in the United States: clinical signs, lesions, and viral genomic sequences. *J Vet Diagn Invest*. 2013;**25**:649–654.
36. Summers BA, Cummings JF, de Lahunta A. *Veterinary Neuro-pathology*. Saint Louis, MO: Mosby; 1995.
37. Tracy ML, Moeller G. Continuous flow vapor generation for inductively coupled argon plasma spectrometric analysis: part 1. Selenium. *J Assoc Off Anal Chem*. 1990;**3**:404–410.

38. Wege H, Siddell S, Ter Meulen V. The biology and pathogenesis of coronavirus. *Curr Top Microbiol Immunol*. 1982; **99**:165–200.
39. Woc-Colburn AM, Garner MM, Bradway D, et al. Fatal coxiellosis in Swainson's Blue Mountain Rainbow Lorikeets (*Trichoglossus haematodus moluccanus*). *Vet Pathol*. 2008; **45**:247–254.
40. Woo PC, Lau SK, Huang Y, et al. Coronavirus diversity, phylogeny and interspecies jumping. *Exp Biol Med*. 2009; **234**: 1117–1127.
41. Woo PC, Lau SK, Lam CS, et al. Discovery of seven novel mammalian and avian coronaviruses in the genus Deltacoronavirus supports bat coronaviruses as the gene source of Alphacoronavirus and Betacoronavirus and avian coronaviruses as the gene source of Gammacoronavirus and Deltacoronavirus. *J Virol*. 2012; **86**:3995–4008.
42. Woods LW, Hanley RS, Chiu PH, et al. Lesions and transmission of experimental adenovirus hemorrhagic disease in black-tailed-deer fawns. *Vet Pathol*. 1999; **36**:100–110.
43. Zaki AM, van Boheemen S, Besterbroer TM, et al. Isolation of a novel coronavirus from a man with pneumonia in Saudi Arabia. *N Engl J Med*. 2012; **367**:1814–1820.
44. Zhang J, Guy JS, Snijder EJ, et al. Genomic characterization of equine coronavirus. *Virology*. 2007; **369**:92–104.
45. Zhang Y, Wang L, Hayes JR, et al. Histological lesions in piglets associated with a swine Deltacoronavirus. Paper presented at: American Association of Veterinary Laboratory Diagnosticians; October 2014; Kansas City, MO.